Article | Received 4 September 2025; Revised 27 November 2025; Accepted 25 December 2025; Published 19 January 2026
https://doi.org/10.55092/am20260003

Effect of reflow profile on reliability of CNT-composite solder joint

Seri Rahayu Kamat[1], Intan Fatihah Ahmad[2,*], Rudi Setiawan[3] and Syamimi Shamsuddin[4]

[1] Department of Industrial Engineering, Faculty of Industrial and Manufacturing Technology and Engineering, Universiti Teknikal Malaysia Melaka, 76100 Durian Tunggal, Malaysia
[2] Centre for Advanced Materials, Faculty of Engineering and Technology, Tunku Abdul Rahman University of Management and Technology (Main Campus), 53300 Kuala Lumpur, Malaysia
[3] Department of Biomedical Engineering, Institut Teknologi Sumatera, 35365 Lampung, Indonesia
[4] Department of Community Health, Advanced Medical and Dental Institute, Universiti Sains Malaysia, 13200 Kepala Batas, Malaysia

* Correspondence author; E-mail: intanfatihah@tarc.edu.my.

Highlights:

- CNT lowers melting activation energy without shifting SAC305 melting point.
- DSC confirms reduced fusion enthalpy in CNT-reinforced SAC305 solder.
- Longer time-above-liquidus enhances wetting and surface uniformity.
- 150 s reflow produces uniform IMC and lowest contact angle.
- Reflow duration is critical for CNT-composite solder joint reliability.

Abstract: This study investigates the effect of the different wt % of carbon nanotube (CNT) on melting point and the effect of time duration in the reflow zone on the reliability of the CNT-composite solder (CCS) solder. The reliability of the CCS solder was evaluated based on the microstructure and wettability of the CCS solder. The CCS with different wt % of CNT was first characterized with Differential Scanning Calorimetry (DSC) to obtain the melting point of the solder. Meanwhile, the microstructure and wettability of the solder were observed through SEM and ImageJ. The results show that the addition of the CNT within the solder matrix will not affect the melting point of the solder. However, a long duration of time within the reflow zone would improve the microstructure and wettability of the CCS solder.

Keywords: CNT-composite solder; reflow profile; carbon nanotube; intermetallic compound

1. Introduction

The interconnect plays a significant role in increasing the performance of the electronic device [1]. After Pb was banned, many researchers have focused on Sn-Ag-Cu (SAC) alloy as their mark as the compatible solder alloy among lead-free solder alloy [2]. At present, the demands on the miniature electronic package have increased, which has raised attention from the manufacturer on several predicaments, especially the interconnect reliability within the miniature electronic package. To solve the issues, the researcher pays interest in the composite solder where the existing binary or tertiary solder was mixed with the rare earth element, metal-based element [3,4], ceramic material [5,6], or carbon-based material [7]. Among all the materials, the carbon-based material has been a popular material to be mixed into the solder matrix due to its excellent wetting in the solder matrix [8] and its ability to improve the solder's mechanical and thermal properties without affecting the electrical properties [9].

The researcher has embarked on numerous studies on the commercial solder mixed with the carbon-based solder, but the research on the suitable profile to use when reflowing the mixed solder has not been conducted. The reflow profile was important as it would affect the solder joint's intermetallic compound (IMC) formation [10]. The reflow profile is usually used during the reflow process to create the solder joint. The profile consists of four zones, which are preheating, soaking, reflow, and cooling [11]. Among all the zones, the reflow zone was the most essential as the joint between the solder and the substrate will be formed by generating the IMC at the solder/substrate interface [12]. Jianbiao *et al.* [13] state that the good profile can be evaluated by observing the IMC formation of the solder joint and the wetting of the solder. The IMC would only be generated when the solder has enough time to melt and interact with the surface's substrate.

In this study, the commercial solder with type SAC 305 will be mixed with different wt % of CNT to form composite solder. The reason was to identify the effect of the amount of CNT added into the solder matrix before identifying the suitable reflow profile for the CNT-composite solder. The changes in the intermetallics and solder wetting were investigated.

2. Experimental procedure

There are two essential parameters in the reflow profile: heating temperature and duration of the sample exposure to the heating temperature. The heating temperature refers to the temperature of preheating, soaking, and reflow. Among all the zones, the reflow temperature, which is also called time above liquidus (TAL), was the most critical zone [13]. The TAL zone is essential because it could affect the microstructure and width of IMC [14]. During this zone, the solder was exposed to a high allowable temperature in the entire process. The TAL acquires solder paste to be heated with an additional 20–40 °C above the solder's liquidus temperature to ensure the solder completely melts before solidifying to reduce solder joint brittleness. Theoretically, the mixture of different types of material will have a different melting temperature (T_m). Different T_m of material will require a new reflow profile to avoid component reliability concerns [13].

There, the preparation of the sample will be divided into two stages. The first stage was preparing the sample CCS paste subjected to different wt % of CNT. The second stage was preparing a sample to identify the effect of time duration during the reflow zone.

2.1. Preparation of the sample

The preparation of the CNT-composite solder for stage 1 and stage 2 was the same. The multiwalled carbon nanotube (MWCNT) nano-powder with a diameter of 10 to 20 nm and length from 0.5 to 2 μm by Sigma Aldrich was used to prepare the CNT-composite solder. The CNT will be added into the commercial SAC 305 solder alloy paste at a nominal weight percentage (wt %) of 0.01, 0.02, 0.03, and 0.04. A no-clean rosin mildly activated (RMA) flux was used throughout the soldering and reflow processes to promote oxide removal and improve wetting during melting. The mixture was agitated using a paste mixing machine (Thinky mixer, ARE-310) for 400 s with 1000 rpm to produce the CCS. The CCS paste that is added with different wt % of CNT will be characterised with DSC to identify the thermal behaviour of each paste by comparing it with the commercial SAC 305 solder alloy.

After the identification is complete, the CCS, which contains 0.04 wt % of CNT (0.04-CCS), will be manually put on the substrate using the syringe. The substrate used in this study was a positive resist-coated circuit board (PCB). The copper layer on the PCB was altered into a circular shape with a diameter of 3 mm. The PCB underwent a PCB fabrication process, which it starts with the ultraviolet (UV) curing process, developing process, etching process, and photoresist stripper process. After the 0.04-CCS was placed on the PCB, the 0.04-CCS will undergo a reflow process, but with three different reflow profiles. The 0.04-CCS that uses profile one will be named as sample 1. Meanwhile, the 0.04-CCS using profile two and profile three will be named sample 2 and sample 3. The time duration at the reflow zone was different for all profiles, where profile one was 60 s, profile two was 105 s, and profile three was 150 s. However, the ramp-up rate, soaking temperature, peak temperature and cooling rate are the same for all profiles with 3 °C/s, 150 °C, 245 °C and 6 °C. The details of the process flow are shown in Figure 1, and the details of all three profiles are shown in Figure 2.

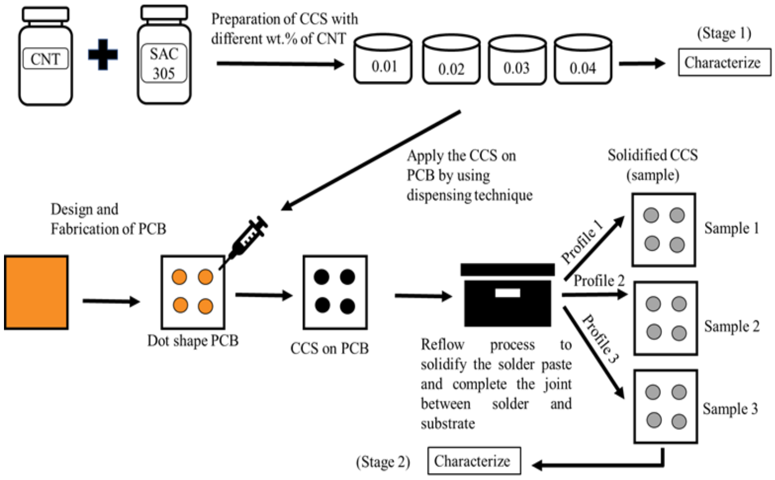

Figure 1. Process of sample preparation.

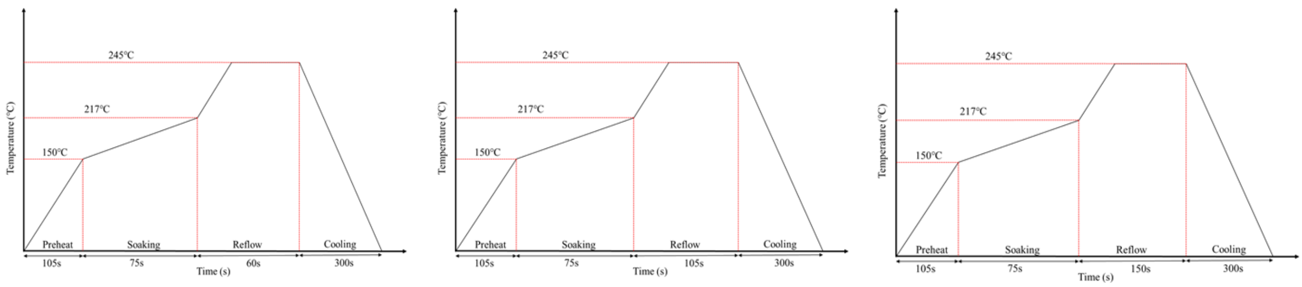

(a) (b) (c)

Figure 2. Three profiles with different durations of reflow time: **(a)** Profile one with 60 s; **(b)** Profile two with 105 s; **(c)** Profile three with 150 s.

2.2. Characterization of the composite solder

The CCS with different wt % of CNT was characterized with DSC (DSC 4000, Perkin Elmer USA) to identify the effect of different wt % of CNT added into the solder matrix. The CCS sample was heated and cooled two times (two cycles) to avoid volatility in DSC results. The sample was heated from 25 °C to 245 °C at a heating rate of 0.05 °C/min. The analysis was carried out with the nitrogen gas atmosphere at a 20 mL/min gas flow.

For metallographic observation, the samples will first be cold-mounted with epoxy resin and hardener with a ratio of 3:1 before being left to harden for a day. Then, the samples will be mechanically cross-sectioned by a metallographic polisher machine, starting with silicon carbide paper grit sizes of 180, 320, 600, and 1500 together with running distilled water. Afterwards, the ground sample will be polished using 6, 3, and 1 µm DIAMAT™ Polycrystalline Diamond suspension, followed by 0.05 µm NANOPOLISH Alumina. Finally, the sample will be etched with a mixture of 2% Hydrochloric acid (HCL), 5% Nitric acid (HNO_3), and 93% methanol for a few seconds. All of the metallographic images were taken using JEOL JSM-IT300 SEM with back-scattered (BSE) mode.

3. Result and discussion

3.1. Thermal behavior of CNT-composite solder

The CCS with different wt % of CNT underwent thermal analysis using the DSC machine to check whether the T_m of the solder SAC305 has changed after adding CNT. Figure 3 shows the DSC profile of SAC305 solder alloy. The profile depicted apparent endotherm peak and exotherm peak, where the endotherm peak shared the solder's melting point information, and the exotherm peak shared the solder's crystallization point. The CCS with different wt % of CNT (0.01-CCS, 0.02-CCS, 0.03-CCS, and 0.04-CCS) also has a similar DSC profile with the SAC305 profile, which only shows the endotherm peak and exotherm peak.

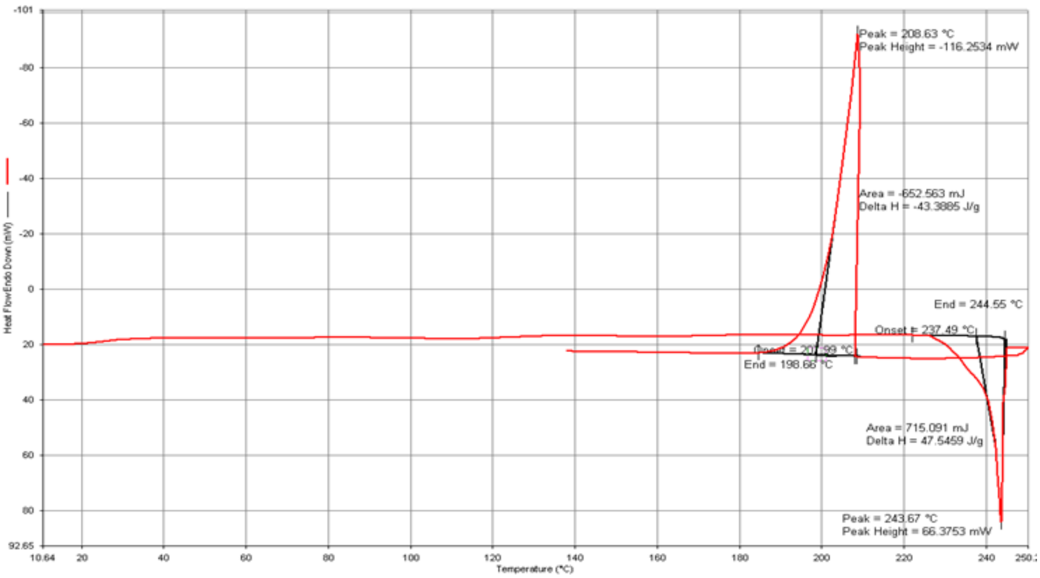

Figure 3. The DSC profile of solder SAC305.

Figure 4 enlarges the endothermic peak of five types of solder: SAC305, 0.01-CCS, 0.02-CCS, 0.03-CCS, and 0.04-CCS. It shows that all of the solder has a similar graph pattern. The graph depicted the peak melting temperature (T_{pm}) and onset melting temperature (T_{om}) of all five solder types. The T_{om} is the beginning temperature for solder starts to melt and is called the solidus temperature [15]. Therefore, the T_{om} in the DSC profile is usually taken as the melting temperature (T_m) [16]. The T_m value of the SAC305 increased as much as 0.35 °C, 0.91°C, 1.02 °C, and 4.58 °C as 0.01, 0.02, 0.03, and 0.04 wt % of CNT added to the SAC305. Similarly, the T_m value of CCS has increased by at most 1.8 %, and the shift remains small and does not indicate a meaningful change in the melting point of SAC305.

Meanwhile, the T_{pm} is a temperature where the solder has completely melted (liquidus temperature). The T_{pm} value for SAC305, 0.01-CCS, 0.02-CCS, 0.03-CCS and 0.04-CCS were 243.62 °C, 243.71 °C, 243.97 °C, 244.05 °C and 244.23 °C. The T_{pm} for all five solders has increased, but with a relatively small value, with the increased value being less than 1 °C. The possible reasons for the T_{om} and T_m of CCS to increase are the reduction in the surface instability with the lower surface free energy rendered by the addition of CNT [17].

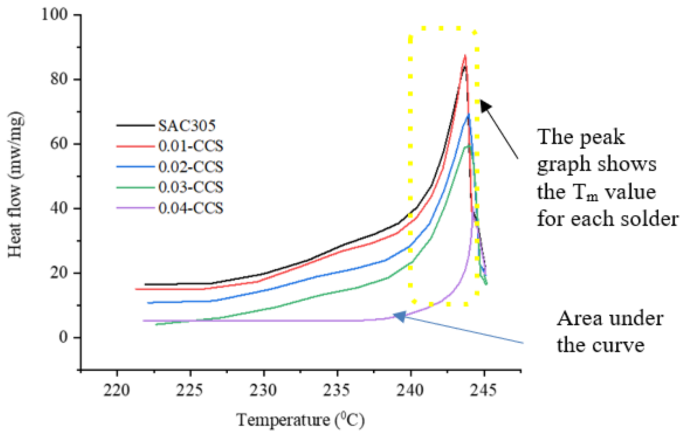

Figure 4. Endothermic graph of SAC305 and CCS solder.

Besides lowering the surface free energy, the CNT can also reduce the energy required by the solder to activate the chemical reaction (change the matter of the solder from paste to liquid), which is also called activation energy (E_{Am}) [18]. The fusion enthalpy (ΔH_m) and activation energy (E_{Am}) were determined to understand the effect of CNT on the energy required for phase transition. The fusion enthalpy was calculated from the area under the endothermic melting peak as shown in Figure 4 [19], normalised by the sample mass, using the equation below;

$$\Delta H_m = \frac{1}{m}\int_{T_1}^{T_2}(\frac{dQ}{dT})dT \tag{1}$$

Where m is the sample mass, $\frac{dQ}{dT}$ is DSC heat flow, and T_1 to T_2 is the temperature range of melting.

Similarly, the activation energy for melting was estimated from the total area under the endothermic curve, which reflects the energy needed for atomic mobility during melting;

$$E_{Am} \propto \int_{T_1}^{T_2}\left(\frac{dQ}{dT}\right)dT \tag{2}$$

The detailed value of E_{Am} is shown in Table 1. Table 2 shows that the E_{Am} for SAC305 was 941.903 mJ, and the value drops to 706.904 mJ, 590.526 mJ, 517.482 mJ, and 496.555 mJ as 0.01, 0.02, 0.03, and

0.04 wt % of CNT added into the solder. It is noticed that the value of E_{Am} was inversely proportional to the amount of the CNT added into the SAC305 solder.

Table 1. Solidus, liquidus, and melting range of the SAC305 solder alloy and CCS.

Materials	°C	
	T_{om}	T_{pm}
SAC305	237.30	243.62
0.01-CCS	237.65	243.71
0.02-CCS	238.21	243.97
0.03-CCS	237.32	244.05
0.04-CCS	241.88	244.23

Table 2. Thermal properties of SAC305 solder alloy and CCS.

Solder alloys	The heat of Fusion (J/g) ΔH_m	Area of the curve (mJ) E_{Am}
SAC305	62.6266	941.903
0.01-CCS	59.9631	706.904
0.02-CCS	59.0526	590.526
0.03-CCS	54.6867	517.482
0.04-CCS	50.8564	496.555

The E_{Am} was related to the rate of the chemical reaction. The rate of the chemical reaction was the rate of the atoms within the solder to break the intramolecular attraction between each other. It shows that 0.04-CCS has the highest reaction rate compared to 0.03-CCS, 0.02-CCS, 0.01-CCS, and SAC305. Meanwhile, the SAC305 has the lowest reaction rate compared to other solders. The intramolecular attraction referred to the attraction between atoms within the solder, as depicted in Figure 5a.

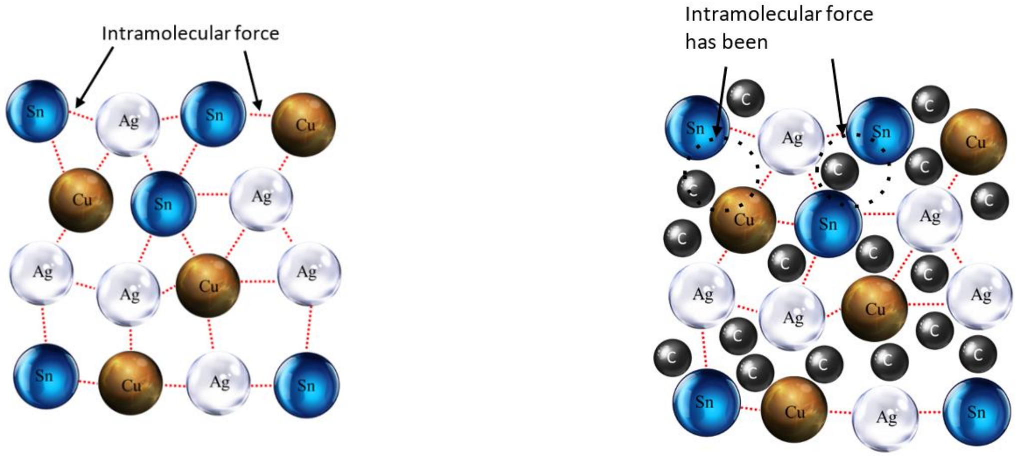

(a) (b)

Figure 5. Illustration of **(a)** intermolecular force within solder alloy system and **(b)** intermolecular force within a composite solder system.

The SAC305 contains the tiny ball of Sn atoms, Ag atoms, and Cu atoms, and these atoms are bonded to each other by the metallic bond. This bonding is a strong bonding among all types of intramolecular forces [20]. Therefore, the solder needs high energy to break the bond. Different from the SAC305 solder, the CCS contains the CNT. CNTs are cylindrical nanostructures composed of sp^2-bonded carbon arranged in a graphitic lattice. In this study, the presence of CNTs within the solder matrix was confirmed through EDS analysis, as shown in Figure 6, which detected carbon peaks in CNT-reinforced samples. These carbon signals were absent in the plain SAC305 solder, indicating that CNTs were successfully incorporated into the composite solder. Figure 5b illustrates that the carbon nanotubes will form a weak van der Waals force with the Sn, Ag, or Cu because of their graphitic sp2-bonded carbon structure [21]. When CNTs are introduced into the SAC305 matrix, they create nanoscale interfaces where the metallic Sn-Ag-Cu bonding network is physically interrupted. This interfacial region contains weaker metallic bonds compared to the bulk solder. As a result, less energy is required to initiate atomic mobility during melting [22]. This behaviour is confirmed by the reduction in fusion enthalpy (ΔHm) and activation energy (EAm)observed in this study. The fusion heat (ΔH) provides information on the amount of heat absorbed during the change of a material from a solid or paste to a liquid [23]. The decrease in ΔHm indicates that fewer strong bonds need to be broken during melting, while the reduction in EAm suggests that atomic rearrangement becomes energetically easier due to the presence of CNT-metal weak interactions. Additionally, adding more CNT into the solder will cause the bonding between the solder to break easily. This statement explained why the 0.04-CCS required the lowest fusion heat compared to 0.03-CCS, 0.02-CCS, 0.01-CCS, and SAC305. Table 1 depicts the heat of fusion for SAC305, 0.01-CCS, 0.02-CCS, 0.03-CCS and 0.04-CCS. The table shows that the fusion heat for SAC305 was highest with 62.6266 J/g, and the heat decreased to 59.9631 J/g, 59.0526 J/g, 54.6867 J/g, and 50.8564 J/g as 0.01, 0.02, 0.03, and 0.04 wt % of CNT added into the SAC305. Therefore, the observed changes in melting energetics arise from CNT-induced modification of the local bonding environment rather than from a significant shift in the composite's melting temperature.

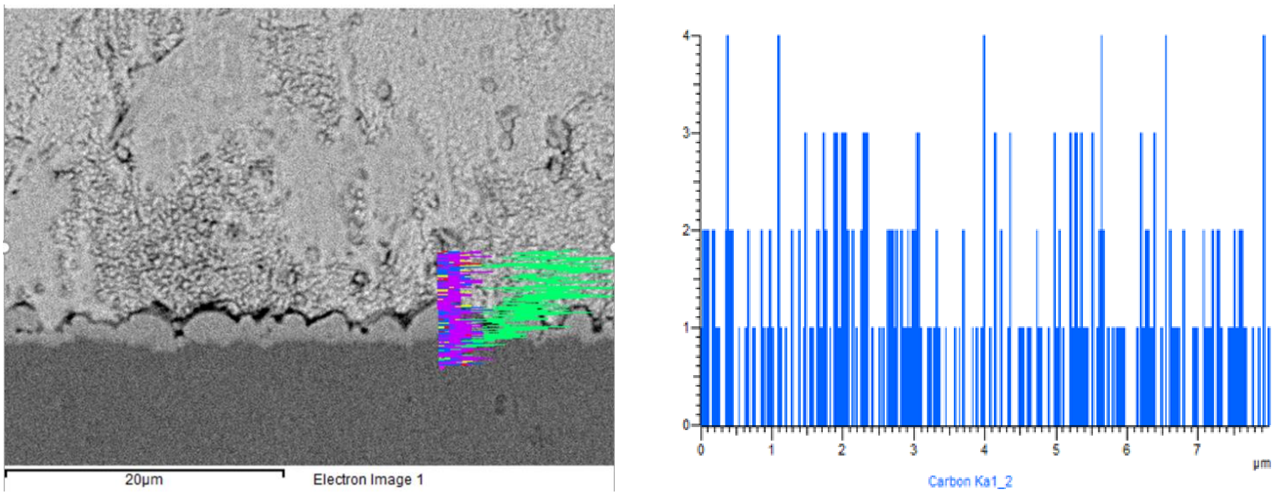

(a) (b)

Figure 6. The EDS results for 0.04-CCS **(a)** the microstructure of the IMC; **(b)** the carbon spectrum.

The Institute for Printed Circuits/Joint Electron Device Engineering Council (IPC/JEDEC) joint industry-standard: J-STD-020D suggested the reflow temperature to be 20 °C to 30 °C higher than melting temperature. The main reason was to ensure the solder melted and interacted with the substrate to form a joint. The T_{pm} value from the DSC profile already shows the optimum temperature needed to melt the entire solder. Although the CNT percentage incorporated in the SAC305 solder will cause the T_{pm} to increase, the increasing value was relatively small. The increasing value of T_{pm}, which is less than 1 °C, shows that the CNT's addition did not significantly affect the SAC305. Therefore, the peak reflow temperature for the CCS will be used as recommended by IPC-JEDEC, which is 245 °C. The decision was made because the T_{pm} of CCS did not exceed the recommended peak temperature by IPC-JEDEC. However, to ensure the best reflow profile for composite solder, further investigation was made to find the CCS's ideal duration time to expose the reflow temperature.

3.2. Ideal duration of exposure reflow temperature for CCS reflow profile

The experiment to determine the ideal duration of exposure at the reflow temperature was conducted using only the 0.04-CCS sample. This sample was selected because the DSC results showed that the peak melting temperature of all CCS composites was similar, while the 0.04-CCS exhibited the highest chemical reaction rate. Salam *et al.* [10] reported that excessive heat exposure during the reflow zone promotes excessive IMC growth, whereas insufficient duration may trap moisture inside the solder and lead to cracking [24].

Three reflow durations were tested: 60 s, 105 s, and 150 s were chosen based on the range recommended by the IPC/JEDEC joint industry standard. All profiles shared identical temperature settings and exposure periods for each zone, except for the duration of the reflow zone. Figure 2 shows the reflow profiles used in this experiment. The CCS reflowed for 60 s was designated as Profile 1, while those reflowed for 105 s and 150 s were designated as Profile 2 and Profile 3, respectively. Pan *et al.* [13] conducted a similar study on SAC305 and reported that the optimal reflow duration results in higher shear strength of solder joints, which is closely associated with improved wetting. Therefore, in this study, the optimal duration was determined based on the solder exhibiting the best wetting behaviour.

Figure 7 presents the top-view micrographs of 0.04-CCS after reflow using Profiles 1, 2, and 3. By comparing the three conditions, the surface of the solder in Profile 1 appeared densely populated with tiny spherical particles, with an average diameter of approximately 1.074 µm. In Profile 2, these particles were fewer, and the average diameter decreased to about 0.877 µm. Particle sizes were measured using ImageJ on optical micrographs that had been previously calibrated using the embedded scale bar. Measurements were obtained using the area-equivalent circular diameter function, and the reported values reflect the converted micrometre units produced by ImageJ's calibrated settings. However, no such particles were observed on the surface of the sample processed using Profile 3, although the surface appeared rough and clumped.

The tiny spherical particles observed in Profile 1 are interpretend as unmelted solder balls that did not fully liquefy during the reflow process. Tian *et al.* [25] reported similar observations, attributing the presence of these particles to insufficient reflow duration, which prevented complete melting. In their study, flux evaporation increased the viscosity of the solder, further hindering full melting. Figure 8 illustrates the mechanism responsible for these particles. During reflow, the solder begins melting at approximately 241.88 °C (refer to Table 1), while the flux simultaneously starts to evaporate. Complete melting should occur near 245 °C; however, the short exposure at this temperature in Profile 1 prevented full melting. During cooling, the partially melted solidified and bound the remaining unmelted particles together. This mechanism also explains the reduction in particle diameter in Profile 2. In contrast, in Profile 3, the longer time above the liquidus allowed sufficient time for all fine solder particles to melt and interact before solidification, resulting in a clumped and more uniform surface.

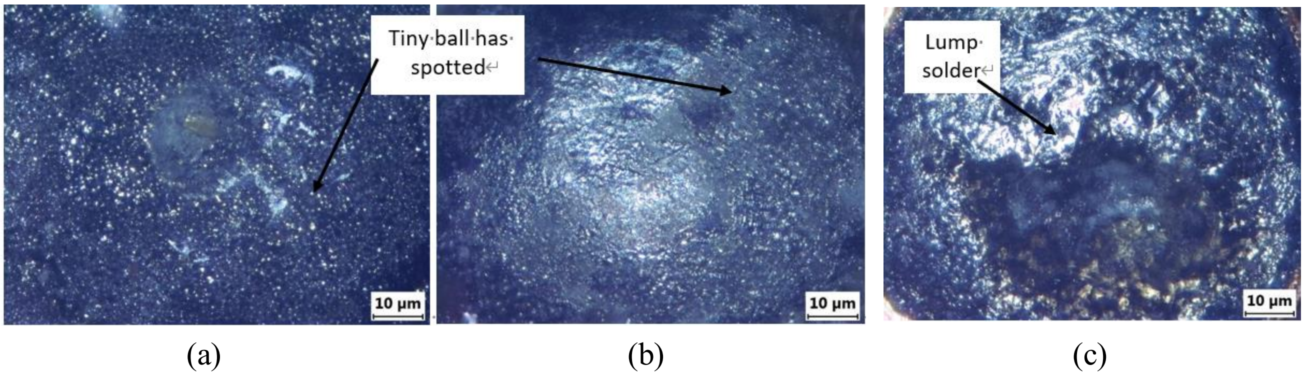

Figure 7. Top view of 0.04-CCS after using **(a)** profile 1 **(b)** profile 2 **(c)** profile 3.

Although gas evolution from the molten solder can also generate voids, several observations in this study indicate that this was not the primary mechanism. The voids and lumpy structures observed in Profiles 1 and 2 were rounded and irregular, which are features commonly associated with trapped flux rather than gas escape. Gas-escape voids usually appear as elongated or directional channels because the gas migrates toward the outer surface as the solder cools, which was not observed in any of the samples. In contrast, the short TAL in Profiles 1 and 2 limited the volatilisation of flux, resulting in incomplete flux removal and insufficient melting of the smaller solder particles. This explanation is supported by the presence of tiny residual balls on the surface of 0.04-CCS, similar to the findings reported by [26], who also attributed such features to insufficient melting time during reflow. Therefore, the voids and lumpy morphology in Profiles 1 and 2 are attributed to trapped flux and incomplete melting rather than gas escape from the solder melt.

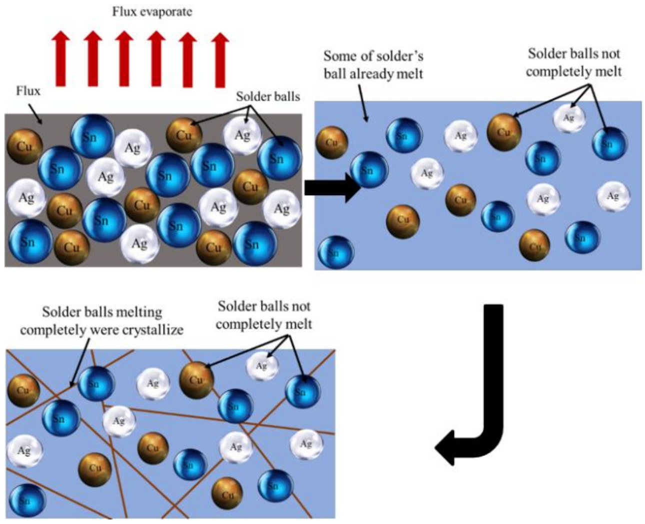

Figure 8. Illustration of the process of the tiny ball appearing after the reflow process.

In summary, profile 3 shows the best reflow profile for CCS compared to the other two. However, the decision was made based only on morphological observation. Therefore, an additional study on wetting behavior and forming the intermetallic compound for all samples was carried out to support the findings.

All samples' wetting behavior was determined by measuring the contact angle (ϴ°) between composite solder and Cu substrate. A good wetting elucidates better adhesion between composite solder and copper substrate, represented by a small value of contact angle [27]. Meanwhile, poor wetting was implied by the high contact angle value. Figure 9 shows the contact angles measured for 0.04-CCS that used profile 1, profile 2, and profile 3 acknowledged as sample 1, sample 2, and sample 3. The contact angle for sample 1 has been found to be 63.5°, while the contact angle for sample 2 has been found to be 45.4°, and the contact angle for sample 3 has been found to be 35.3°. Succinctly, the composite solder's contact angle decreased when the duration of time in the reflow zone increased. Ramli *et al.* [28] stated that a contact angle value below 45º is considered good wettability. Thus, profiles 2 and 3 were considered to give a good wetting for 0.04-CCS during the reflow process.

The almost complete spreading of 0.04-CCS under Profile 3, as evidenced by the lowest contact angle and absence of unmelted particles, indicates superior wetting behaviour when compared to Profiles 1 and 2. In industry and academic literature, enhanced wetting correlates strongly with improved metallurgical bonding, reduced void content and greater mechanical integrity of solder joints [13,29]. Accordingly, the combination of CNT addition and optimised time-above-liquidus contributes not only to microstructural refinements but also sets the stage for enhanced solder joint properties.

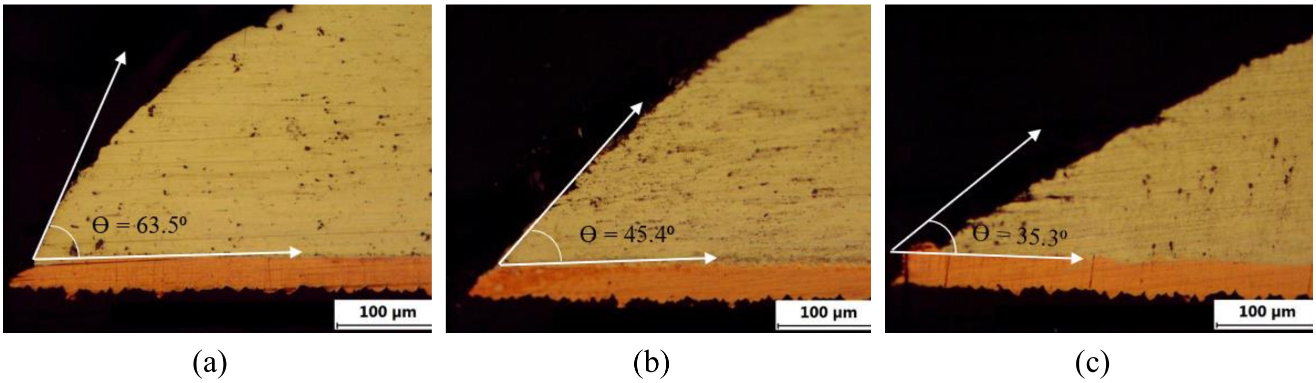

Figure 9. Contact angle measurement for 0.04-CCS reflow under **(a)** profile 1 **(b)** profile 2, and **(c)** profile 3.

The cross-sections of samples 1, 2, and 3 were observed through the scanning electron micrography (SEM) equipment for better insight into this explicit event. Figure 10 depicts the backscatter image of sample 1, sample 2, and sample 3. The cross-section for sample 1 seems to have a rough surface. The rough surface was due to the significant lump fills on the solder's surface, as shown in Figure 10a. The IMC formation in sample 1 verifies that the solder has successfully joined the substrate during the reflow process. However, the quality of the joint was poor through the gap along the IMC's top. The void and the gap were also spotted in sample 2, as illustrated in Figure 10b. The gap was smaller than in sample 1, and the solder's surface was also smoother than sample 1. Sample 3 seemed to have a smoother surface, with the IMC properly intact with the solder.

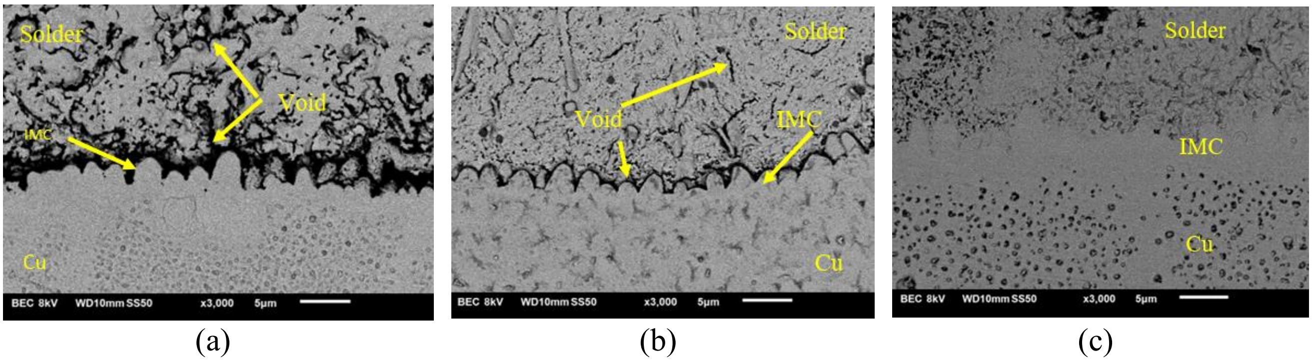

Figure 10. Backscatter image of 0.04-CCS with **(a)** sample 1 **(b)** sample 2 **(c)** sample 3.

The formation of the void can be related to the different durations of reflow temperature exposure. Sample 3 was exposed to the reflow temperature longer than samples 2 and 1. This statement explained that sample 3 stayed in liquid form longer compared to the other samples. During that duration, the solder's volatile flux was not soluble in molten solder and would evaporate. The evaporated flux will be climbing up to the molten solder's surface in the gases form. The long-duration sample 3 stayed in liquid form, which would give the flux enough time to be completely evaporated. Meanwhile, sample 2 stayed in a liquid form shorter than sample 3, and sample 1 stayed in a liquid form the shortest compared to the other two samples. The formation of void happens because the volatile flux does not have enough time to escape from the molten solder. Therefore, the trapped flux would create the void [29]. A similar phenomenon was reported by other researchers [30], where the effect of the different reflow profiles was studied on four types of solder. In that study, it was concluded that the formation of the void happens due to the solder staying in liquid form for a short duration, which leads to the gas not having enough time to escape.

CNT also serve as a physical barrier to atomic diffusion during the formation of IMCs. Their presence reduces the continuity of the Sn-Ag-Cu reaction pathway by introducing non-reactive graphitic interfaces. This effect contributes to the observed refinement of the IMC layer and supports the reduced bonding strength inferred from the thermal analysis.

Table 3 summarises the findings of the experiment on different times of reflow temperatures. In summary, profile 3 was the best choice among all the profiles. Although through the primary observation, the 0.04-CCS's surface was seen to have a clumped surface by detailed observation using SEM equipment shows that the sample has a smoother surface compared to the sample using another profile. On top of that, give a good wetting on the sample.

Table 3. Summary findings of experiment on different time of reflow temperature.

	Morphological observation through Upright microscope	**Wetting behavior**	**Intermetallic compound observation through SEM**
Sample 1 (Profile 1)	A dense tiny ball was spotted on the solder's surface.	Not good	Porosity and there was a gap between IMC and solder.
Sample 2 (Profile 2)	Less dense with a smaller diameter of tiny ball was spotted on the solder's surface.	Good	The surface becomes smoother, and the gap between IMC and solder has reduced.
Sample 3 (Profile 3)	Clump surface.	Good	The surface was smoother compare to other samples.

3.3. Summary of CCS reflow profile

The IPC/JEDEC joint industry-standard: J-STD-020D suggested the reflow temperature to be 20 °C to 30 °C higher than the melting temperature. The main reason was to ensure the solder melted and interacted with the substrate to form a joint. However, the T_{pm} value from the DSC profile already shows the optimum temperature needed to melt the entire solder. The peak temperature will be used on the CCS, similar to the recommendation by IPC-JEDEC, 245 °C. It was because the T_{pm} value of CCS did not exceed the recommended peak temperature by IPC-JEDEC. The detailed reflow profile used on the CCS throughout this study was tabulated in Table 4.

Table 4. Details information on reflow profile used on CCS solder.

Profile Feature	CCS temperature and duration of time
Average Ramp-Up rate	3 °C/second
Preheat	
Temperature	150 °C
Time	105 s
Peak Temperature	245 °C
Time	150 s
Ramp-Down rate	6 °C/second

4. Conclusions

Two major findings can be concluded from the study:

(1) This study concludes that adding the CNT to the SAC305 solder matrix shows small increases in the onset melting temperature and peak temperature; however, the magnitude of these changes is very small and does not represent a meaningful shift in the melting behavior of the alloy. The T_{pm} values for all CNT compositions remain essentially within the same temperature range recommended for SAC305 reflow processes. Therefore, the solder still melts at the same practical temperature from a reflow manufacturing perspective. Despite all, the CNT still does significantly change towards energy required for the solder to transition from solid to liquid, as shown by the reduction in activation energy (E_{Am}) and fusion enthalpy (ΔH_m). This indicates that the CNT weaken the interactions among Sn, Ag, and Cu atoms, making the alloy easier to melt even though the nominal melting temperature remains effectively unchanged. In other words, CNTs influence the melting kinetics rather than the melting point.

(2) Although the melting temperature remains practically unaffected, the duration of the reflow zone strongly influences the joint quality. A time above liquidus of 150 s resulted give the composite solder having smoother microstructures, the most uniform IMC layer, and the best wettability performance. The improved contact angle and the absence of Sn-rich particles confirm that extended TAL enhances spreading and stabilises interfacial reactions in CNT-reinforced solder joints.

These findings show that the CNT addition modifies the energy characteristics and interfacial behavior of the solder, while an optimised reflow duration governs the physical microstructure and reliability of the CNT-composite solder joints. While direct mechanical testing (e.g., shear strength, fatigue life) was not conducted in this study, the observed microstructural features—namely the refined intermetallic compound layer, absence of unmelted particles, and improved wetting—are predictive of enhanced joint performance. Prior work on CNT-reinforced Sn-based solders has demonstrated improved creep resistance and shear strength in joints with comparable microstructure [30]. Therefore, it is reasonable to expect that the 0.04-CCS solder processed under Profile 3 will yield mechanical and reliability improvements. Future work should include mechanical and reliability testing to quantify these property gains.

This study focuses on DSC analysis and microstructural examination through optical microscopy and SEM, more detailed characterization techniques, such as EDS elemental mapping and XRD-based micro-stress analysis, were not included. These techniques would provide deeper insight into elemental distribution, IMC evolution, and residual stress states. Future work will incorporate these methods to further validate and expand upon the relationships observed in this study.

Acknowledgements

I would like to express my gratitude to Universiti Teknikal Malaysia Melaka (UTeM) for their support in covering the publication fee and facilities provided. This work was conducted independently and did not receive any specific grant. I am also thankful for the resources provided by Tunku Abdul Rahman University of Management and Technology (TARUMT).

Authors' contribution

Intan Fatihah Ahmad: conceptualization, methodology, software, formal analysis and writing—original draft preparation; Seri Rahayu Kamat: data curation, validation, supervision; software, validation, funding acquisition, writing reviewing; Rudi Setiawan and Syamimi Shamsuddin: visualization, writing—reviewing and editing.

Conflicts of interests

The authors declare no conflict of interest.

References

[1] Zeng G, Xue S, Zhang L, Gao L, Dai W, *et al*. A review on the interfacial intermetallic compounds between Sn-Ag-Cu based solders and substrates. *J. Mater. Sci.: Mater. Electron.* 2010, 21(5):421–440.

[2] Tay SL, Haseeb A, Johan MR, Munroe PR, Quadir MZ. Influence of Ni nanoparticle on the morphology and growth of interfacial intermetallic compounds between Sn-3.8Ag-0.7Cu lead-free solder and copper substrate. *Intermetallics* 2013, 3:8–15.

[3] Maslinda K, Anasyida AS, Nurulakmal MS. Effect of Al addition to bulk microstructure, IMC formation, wetting and mechanical properties of low-Ag SAC solder. *J. Mater. Sci.: Mater. Electron.* 2016, 27(1):489–502.

[4] Wernicki E, Gu Z. Effect of Sn nanoparticle additions on thermal properties of Sn-Ag-Cu lead-free solder paste. *Thermochim Acta* 2020, 690:178642.

[5] Yahaya MZ, Ani FC, Samsudin Z, Sahin S, Abdullah MZ, *et al*. Hardness profiles of Sn-3.0Ag-0.5Cu-TiO2 composite solder by nanoindentation. *Mater. Sci. Eng.: A* 2016, 669:178–186.

[6] Lu X, Zhang L, Guo Y, Wang X, Li M, *et al.* Microstructure evolution and thermal, wetting, mechanical properties of SiC nanowires reinforced SAC105 composite solder. *Intermetallics* 2023, 154:107816.

[7] Liyana MHN, Hanim MAA, Sulaiman S, Azlina OS. The effect of CNT and Cu on interfacial intermetallic growth of Sn-Ag-Cu solder. *IOP Conf. Ser.: Mater. Sci. Eng.* 2019, 469(1):012007.

[8] Nai SML, Wei J, Gupta M. Effect of carbon nanotubes on the shear strength and electrical resistivity of a lead-free solder. *J. Electron. Mater.* 2008, 37(4):515–522.

[9] Chellvarajoo S, Abdullah MZ. Microstructure and mechanical properties of Pb-free Sn-3.0Ag-0.5Cu solder pastes added with NiO nanoparticles after reflow soldering process. *Mater. Des.* 2016, 90:499–507.

[10] Salam B, Virseda C, Da H, Ekere NN, Durairaj R. Reflow profile study of the Sn-Ag-Cu solder. *Soldering Surf. Mount Technol.* 2004, 16(1):27–34.

[11] Zhang Z, Kim J, Won D. Statistical-based simulation and reflow profile optimization for improving self-alignment performance—an experimental study. *Soldering Surf. Mount Technol.* 2025, 37(4):258–268.

[12] Zhang J, Zhang L, Huang X, Wu C, Deng K, *et al*. Effect of adding Ni nanoparticles on the melting characteristics, mechanical properties and intermetallic compound growth of Sn58Bi solder. *Soldering Surf. Mount Technol.* 2025, 37(1):60–70.

[13] Pan J, Toleno BJ, Chou TC, Dee WJ. The effect of reflow profile on SnPb and SnAgCu solder joint shear strength. 2006, 18(4):48–56.

[14] Aisha ISR, Ourdjini A, Hanim MAA, Azlina OS. Effect of reflow profile on intermetallic compound formation. *IOP Conf. Ser.: Mater. Sci. Eng.* 2013, 46(1):012037.

[15] Belyakov SA, Gourlay CM. Recommended values for the βSn solidus line in Sn-Bi alloys. *Thermochim Acta* 2017, 654:65–69.

[16] Amin M, Soliman HN, El-Taher AM, Mashaly KB, Ragab M. Investigating the role of multi-walled carbon nanotubes in microstructural evolution, thermal stability, and mechanical performance of Sn-Ag lead-free solder alloys for advanced electronic applications. *Mater. Today Commun*. 2025, 46:112681.

[17] Kumar KM, Kripesh V, Tay AAO. Influence of single-wall carbon nanotube addition on the microstructural and tensile properties of Sn-Pb solder alloy. *J. Alloys Compd.* 2008, 455(1,2):148–158.

[18] Plevachuk Y, Švec Sr P, Švec P, Orovcik L, Bajana O, *et al.* Metal deposited nanoparticles as “bridge materials” for lead-free solder nanocomposites. *Appl. Nanosci.* 2023, 13(12):7387–7397.

[19] Ghanbari E, Picken SJ, van Esch JH. Analysis of differential scanning calorimetry (DSC): determining the transition temperatures, and enthalpy and heat capacity changes in multicomponent systems by analytical model fitting. *J. Therm. Anal. Calorim*. 2023, 148(22):12393–12409.

[20] Fu H, Xiao Y, Song R, Wang Z, Ji H, *et al*. Rapid soldering of flexible graphene assembled films at low temperature in air with ultrasonic assistance. *Carbon* 2020, 158:55–62.

[21] Sun H, Chan YC, Wu F. Reliability performance of tin–bismuth–silver (Sn57.6Bi0.4Ag) solder joints with different content of carbon nano-tubes (CNTs) or nickel (Ni)-modified CNTs. *J. Mater. Sci.: Mater. Electron.* 2018, 29(10):8584–8593.

[22] Li L, Qin W, Mai B, Qi D, Yang W, *et al.* Effect of carbon nanotubes on the mechanical, thermal, and electrical properties of Tin-based lead-free solders: a review. *Crystals* 2023, 13(5):789.

[23] Kumar RS, Krishna DJ. Differential Scanning Calorimetry (DSC) analysis of latent heat storage materials for low temperature (40–80 °C) solar heating applications. *IJERT* 2013, 2(8):429–455.

[24] Huang YE, Hagen D, Dody G, Burnette T. Effect of solder reflow temperature profile on plastic package delamination. In *Twenty Third IEEE/CPMT International Electronics Manufacturing Technology Symposium (Cat. No.98CH36205)*, Austin, USA, October 21, 1998, pp. 105–111.

[25] Tian Y, Chan YC, Lai JKL, Pak STF. The effect of solder paste viscosity on porosity and mechanical properties of surface mount solder joints. *IEEE Trans. Compon. Packag. Manuf. Technol: Part B* 1997, 20(2):146–151.

[26] Ahmad IF, Omar G, Kamat SR, Shamsuddin S, Esa SR, *et al*. 2024. Interfacial reaction and intermetallic compound growth behaviour of CNT-filled composite solder on the oxidizing substrate. *J. Adv. Res. Micro Nano Eng.* 2024, 25(1):95–106.

[27] Nai SML, Wei J, Gupta M. Improving the performance of lead-free solder reinforced with multi-walled carbon nanotubes. *Mater. Sci. Eng.: A* 2006, 423(1,2):166–169.

[28] Ramli MII, Saud N, Salleh MAAM, Derman MN, Said RM. Effect of TiO2 additions on Sn-0.7Cu-0.05Ni lead-free composite solder. *Microelectron. Reliab.* 2016, 65:255–264.

[29] Bušek D, Dušek K, Růžička D, Plaček M, Mach P, *et al.* Flux effect on void quantity and size in soldered joints. *Microelectron. Reliab.* 2016, 60:135–140.

[30] Ismail N, Jalar A, Abu Bakar M, Safee NS, Wan Yusoff WY, *et al.* Microstructural evolution and micromechanical properties of SAC305/CNT/CU solder joint under blast wave condition. *Soldering Surf. Mount Technol.* 2021, 33(1):47–56.